ORIGINAL ARTICLE

The Simplest Memristor Oscillator is blessed with an Edge of Chaos Kernel

Maheshwar Sah[1,2] · Vetriveeran Rajamani[3] · Ram Kaji Budhathoki[4] · Devaraj Somasundaram[3] · Sultan Mahmood Chowdhury[3]

Abstract

This paper presents a novel concept that the simplest memristor oscillator designed with the series connection of positive temperature coefficient (PTC) and negative temperature coefficient (NTC) memristors possesses an inherent property referred to as the *"edge of chaos kernel"*, hidden inside the small-signal equivalent circuit serves as an optimal mechanism for inducing a periodic oscillation. Furthermore, it is also demonstrated that the edge of chaos kernel, originated from Chua's riddle and characterized by *negative resistance* ($R < 0$) and *negative inductance* ($L < 0$), exhibits potential stability but becomes unstable upon the addition of dissipative resistance or inductor component. This paper outlines the discoveries concerning the properties and behavior of the edge of chaos kernel circuit in the elementary memristor oscillator as well as the potential application in voltage control sensing circuit, elucidating its significance in nonlinear dynamics.

Keywords Memristor · Edge of chaos kernel · PTC-NTC · Oscillator · Local activity · Local passivity · Edge of chaos · Stable · Unstable

1 Introduction

In the realm of electronic circuits, oscillators play a crucial role in generating repetitive waveforms, a fundamental function in various applications such as signal processing, communications, and timing circuits. The traditional electronics oscillators are designed using energy storage elements, inductors, capacitors along with the locally active nonlinear resistors, transistors and op-amp [1]. The working mechanism of these conventional oscillators are based on the charging and discharging principle of capacitors/inductors and locally active nature of the nonlinear resistors, transistors and op-amp. While traditional oscillators have been widely utilized across various applications, their advancements have reached a maximum-limit due to their complex structures and limitations imposed by transistor sizes. Conversely, the emergence of memristors, a novel fourth circuit element [2, 3] conceptualized by Leon Chua, has sparked significant interest in the development of memristor-based electronic oscillators [4–7]. However, these oscillators typically incorporate memristors with locally active devices, transistors and energy storage components such as capacitors and inductors. On the other hand, we introduced the simplest design of electronic oscillators by utilizing a locally active second-order memristor [8]. This design involves connecting just two "uncoupled" first-order voltage-controlled positive temperature coefficient (PTC) and negative temperature coefficient (NTC) memristors in series, eliminating the need for additional energy storage elements and transistors. Our

✉ Maheshwar Sah
  sahmaheshwar@gmail.com

✉ Vetriveeran Rajamani
  vetriece86@gmail.com

  Ram Kaji Budhathoki
  ramkaji@gmail.com

  Devaraj Somasundaram
  somasundaram.d@vit.ac.in

  Sultan Mahmood Chowdhury
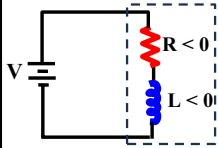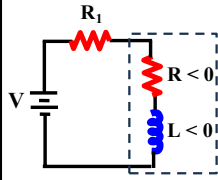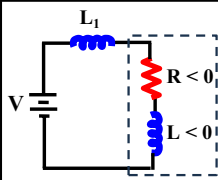 sultan.mahmood@vit.ac.in

[1] Nepal Engineering College, Changunarayan, Bhaktapur, Nepal

[2] TJX, Evansville, IN, USA

[3] School of Electronics Engineering (SENSE), Vellore Institute of Technology, Vellore, Tamilnadu, India

[4] Department of Electrical and Electronics Engineering, Kathmandu University, Dhulikhel, Kavre, Nepal

Table 1 Effects on stability when resistance or inductance is added in the edge of chaos kernel circuit

Case	Circuit	Admittance function	Pole	Stable/Unstable
Case 1	V, $R < 0$, $L < 0$ (circuit diagram)	$Y(s) = \dfrac{1}{Ls + R}$	$s_p = \dfrac{-R}{L}$	Stable
Case 2	R_1, V, $R < 0$, $L < 0$ (circuit diagram)	$Y(s) = \dfrac{1}{(Ls + R + R_1)}$	$s_p = \dfrac{-(R + R_1)}{L}$	Stable: R_1 $|R|$ Unstable: $R_1 > |R|$
Case 3	L_1, V, $R < 0$, $L < 0$ (circuit diagram)	$Y(s) = \dfrac{1}{(Ls + L_1 s + R)}$	$s_p = \dfrac{-R}{(L + L_1)}$	Stable: L_1 $|\ |$ Unstable: $L_1 > |\ |$

simplest model of this oscillator consists of only two differential equations to generate sinusoidal oscillation. The circuit-theoretic analysis and characterizations of this simplest oscillator were presented by small-signal analysis, local activity principle, edge of chaos and Hopf bifurcations theorem. We have shown the memristor oscillator spawns sinusoidal oscillations starting from the either boundary of the edge of chaos regime of the memristor via a super-critical Hopf bifurcation. Though, the waveforms in this oscillator were shown by solving the differential equations, the actual global nonlinear dynamical bifurcations caused by the core circuit hidden inside the small signal model known as edge of chaos kernel that plays an important role to produce oscillation in the simplest model of memristor oscillator was not covered. The term edge of chaos kernel recently introduced by Leon Chua is a simple 1-port electrical circuit in a series connection of *negative resistance (R < 0)* and *negative inductance (L < 0)* which exhibits edge of chaos phenomenon of being potentially stable yet, but unstable when a dissipation is added [9]. Such a shocking and magical events occurred in edge of chaos kernel leads to the generation of action potential in neurons, resolving the Turing's instability and Smale's paradox [10–12]. This is a significant discovery from Chua's riddle that finally succeed to resolve the Galvani's 240-year old unresolved enigma [13]. This paper aims to elucidate and resolve the nonlinear dynamic bifurcations using the powerful 1-port edge of chaos kernel circuit from the small-signal equivalent model of the PTC-NTC memristors oscillator as well as exploring its potential application in the voltage control sensing circuit.

2 Edge of Chaos Kernel

The concept *"edge of chaos kernel"* incarnated from Chua's riddle is the simplest 1-port circuit with negative resistance($R < 0$) and negative inductance ($L < 0$) having potential to create action potential in nature's optimum. The "edge of chaos" is a phase transition region between stable and unstable in a system. The concept "edge of chaos kernel" could be applied to various systems, including electronic circuits like memristors to explore their capabilities at the boundary.

In context of this study, the concept suggests that harnessing the dynamical behavior of memristors at the edge of chaos could lead to novel and efficient approaches for information and computations processing. Table 1 presents comprehensive diverse cases of the edge of chaos kernel circuit. This exploration illustrates a spectrum of scenarios, each offering a unique perspective on how this powerful edge of chaos kernel circuit transforms from stability to instability by adding dissipation of a resistor or an energy storage element inductor[1], revealing a deep understanding of dynamic behavior at the edge of chaos kernel. These cases allow us to uncover how the circuit's dynamics unfold in the presence of small disturbances, offering valuable information about

---

[1] The purpose of showing case 3 in Table 1 is just to provide the information that the addition of a positive inductance can transform the circuit from stable to unstable. The one port circuit is in edge of chaos when the small signal equivalent circuit of a memristor satisfies the condition of $R_1 < 0$, $L_1 < 0$ and $R_a > |R_1|$ as shown in Table 2. Please note that, at least one memristor such as PTC in our case satisfies this condition. This is also known as the signature of the edge of chaos.

its stability, sensitivity, and potential for chaotic behavior. Through these detailed case studies and understanding, we provide the transformative impact of the edge of chaos kernel circuit that sheds light on the potential application in the design of the memristor based electronic oscillator.

3 Edge of Chaos Kernel in the Simplest Memristor Oscillator

Memristors with their unique property to remember the past history serve as the foundational components in oscillator design to generate periodic signals. The distinctive features of these oscillators lie in their purported blessing with an *"edge of chaos kernel"*. This section introduces the crucial role of edge of chaos kernel circuit via the small-signal model of PTC-NTC oscillator to establish a formal proof that the simplest memristor oscillator is blessed with an *"edge of chaos kernel"*.

3.1 PTC-NTC Memristors Oscillator

Positive temperature coefficient (PTC) memristor whose resistance increases as the temperature increases is defined by the following equations [5]:

$$i_1 = G(x_1) v_1 \tag{1a}$$

$$G(x_1) = \left(K_1 e^{\beta_1 (x_1 - \gamma_1)} \right)^{-1} \tag{1b}$$

$$\frac{dx_1}{dt} = \frac{1}{\alpha_1} \left[\delta_1 (\gamma_1 - x_1) + G(x_1) v_1^2 \right] \tag{1c}$$

where K_1, α_1 β_1, δ_1 and γ_1 are the device parameters. The parameters values for the PTC memristor used in this paper are $K_1 = 10^3$, $\alpha_1 = 0.8$, $\beta_1 = 10^4$, $\delta_1 = 0.8$ and $\gamma_1 = 300$.

Similarly, negative temperature coefficient (NTC) memristor whose resistance decreases as the temperature increases is defined by the following equations [14]:

$$i_2 = G(x_2) v_2 \tag{2a}$$

$$G(x_2) = \left(K_2 e^{\beta_2 \left(\frac{1}{x_2} - \frac{1}{\gamma_2} \right)} \right)^{-1} \tag{2b}$$

$$\frac{dx_2}{dt} = \frac{1}{\alpha_2} \left[\delta_1 (\gamma_2 - x_2) + G(x_2) v_2^2 \right] \tag{2c}$$

where K_2, α_2 β_2, δ_2 and γ_2 are the device parameters. The parameters values specified for the NTC memristor are $K_2 = 10^5$, $\alpha_2 = 0.2$, $\beta_2 = 10^7$, $\delta_2 = 0.1$ and $\gamma_2 = 300$.

PTC memristor, characterized by an increase in resistance with rising temperature, and NTC memristor, marked by a decrease in resistance under similar conditions form a compelling duo when connected in series. This configuration, blending the opposing temperature-dependent behaviors of PTC and NTC memristors, holds the promise of creating oscillator with inherent temperature sensitivity and voltage-regulation. The inherent temperature sensitivity of PTC-NTC refers to their ability to exhibit changes in electrical resistance in response to changes in temperature. This sensitivity is an intrinsic property of the material from which the thermistor is made and is typically quantified by the temperature coefficient, which describes how much the resistance changes per unit change in temperature. The nonlinear differential equations associated with the series connection of PTC and NTC memristors are given by following state dependent Ohm's law equations:

$$i = G(x_1, \ x_2) v \tag{3a}$$

$$G(x_1, \ x_2) = \frac{1}{\left(K_1 e^{\beta_1 (x_1 - \gamma_1)} \right) + \left(K_2 e^{\beta_2 \left(\frac{1}{x_2} - \frac{1}{\gamma_2} \right)} \right)} \tag{3b}$$

$$\frac{dx_1}{dt} = \frac{1}{\alpha_1} \left[\delta_1 (\gamma_1 - x_1) + \frac{K_1 e^{\beta_1 (x_1 - \gamma_1)}}{\left(\left(K_1 e^{\beta_1 (x_1 - \gamma_1)} \right) + \left(K_2 e^{\beta_2 \left(\frac{1}{x_2} - \frac{1}{\gamma_2} \right)} \right) \right)^2} v^2 \right] \tag{3c}$$

$$\frac{dx_2}{dt} = \frac{1}{\alpha_2} \left[\delta_2 (\gamma_2 - x_2) + \frac{K_2 e^{\beta_2 \left(\frac{1}{x_2} - \frac{1}{\gamma_2} \right)}}{\left(\left(K_1 e^{\beta_1 (x_1 - \gamma_1)} \right) + \left(K_2 e^{\beta_2 \left(\frac{1}{x_2} - \frac{1}{\gamma_2} \right)} \right) \right)^2} v^2 \right] \tag{3d}$$

The series configuration and its equivalent small-signal model derived using Taylor series expansion and Laplace transform are shown in Fig. 1a and b respectively. The small-signal admittance function and frequency response at an equilibrium point are given by,

$$Y(s; V_Q) = \frac{k(s - z_1)(s - z_2)}{(s - p_1)(s - p_2)} \tag{4a}$$

$$Y(i\omega; V_Q) = \left[\frac{(a_0 - a_2 \omega^2)(b_0 - b_2 \omega^2) + a_1 b_1 \omega^2}{(a_0 - a_2 \omega^2)^2 + a_1^2 \omega^2} \right]$$
$$+ i \left[\frac{[(a_0 - a_2 \omega^2) b_1 - a_1 (b_0 - b_2 \omega^2)] \omega}{(a_0 - a_2 \omega^2)^2 + a_1^2 \omega^2} \right] \tag{4b}$$
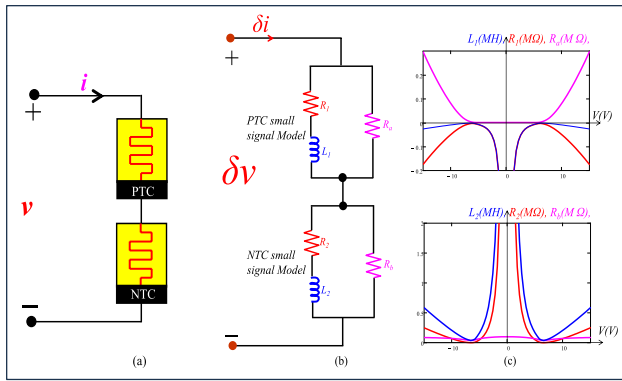
where

Fig. 1 a Series connection of two uncouple first order PTC-NTC memristor. **b** Small-signal equivalent circuit of the PTC-NTC memristors. **c** Inductances and resistances of the small-signal equivalent circuit of the PTC-NTC memristors at the DC equilibrium voltage V

$$
\begin{aligned}
\operatorname{Re} Y(i\omega; V_Q) &= \frac{(a_0 - a_2\omega^2)(b_0 - b_2\omega^2) + a_1 b_1 \omega^2}{(a_0 - a_2\omega^2)^2 + a_1^2\omega^2} \\
\operatorname{Im} Y(i\omega; V_Q) &= \frac{[(a_0 - a_2\omega^2)b_1 - a_1(b_0 - b_2\omega^2)]\omega}{(a_0 - a_2\omega^2)^2 + a_1^2\omega^2}
\end{aligned}
\tag{4c}
$$

The derivations of these equations are omitted here to avoid the clutter. For detailed explanation and coefficient values, readers are encouraged to refer our article [8].

The plots of small signal inductances and resistances L_1, R_1, R_a and L_2, R_2, R_b of the PTC-NTC memristors are shown in Fig. 1c. Observe that the inductance L_1 and resistance R_1 derived from the small signal model of the PTC memristor are always negative for any DC equilibrium voltage V. The negative values of inductance and resistance signify the edge of chaos kernel, representing a range from potentially stable to unstable dynamics. Analyzing this representation offers valuable insights into the system's behavior, emphasizing the significance of the edge of chaos kernel in understanding the stability characteristics of the nonlinear system. The stability characteristics of a nonlinear system involves analyzing how the system responds to disturbances or changes from its equilibrium state. This analysis often utilizes method such as small signal equivalent circuit by linearization of the nonlinear system to determine if the system will remain stable over time or if its behavior will become unpredictable or divergent. This understanding is vital for designing oscillator circuits, control systems and predicting the system's behavior accurately.

Table 2 provides a comprehensive view of the system's behavior via detailed analyses of currents, inductances, resistances, $Re(i\omega; V_Q)$ and poles in response to varying DC voltage levels. Notably, the inclusion of negative inductance (L_1) and resistance(R_1) values signify the presence of an edge of chaos kernel. As the DC voltage varies, the table reveals the dynamic shifts in $Re(i\omega; V_Q)$ and poles, emphasizing critical points where the system makes a transition from a potentially stable state to an unstable state. The presence of negative inductance and negative resistance at the DC equilibrium provides compelling evidence that the PTC-NTC oscillator is endowed with an edge of chaos kernel.

3.1.1 Edge of Chaos Kernel in Locally Passive Regime

A locally passive typically refers to a property where the circuit behaves passively within a certain local region of its operation. The depiction of the edge of chaos kernel within a locally passive regime, highlighted by the blue color in Table 2, presents an intriguing scenario where the inductance(L_1) and resistance(R_1) exhibit negative values. However, the expression $ReY(i\omega; V_Q) > 0$ and the presence of negative poles suggest the stability within the system, particularly aligning with the cases 2 and 3 from Table 1 for the stable condition. This suggests that despite the presence of other positive values of inductances and resistances in the small signal equivalent circuit, the system exhibits stable behavior, indicating a robust stable condition in locally passive regime.

In order to verify the stability condition of PTC-NTC oscillator in a locally passive regime, we have shown the small signal equivalent circuit, the plot of $ReY(i\omega; V_Q)$ vs. ω, and *current*(I) vs. *time*(t), x_2 vs. x_1, in Fig. 2a, b, c and d, respectively at DC equilibrium voltage V = 5.7 V. The numerical computation of corresponding poles (p_1, p_2) with values of $p_1 = -0.1844$ and $p_2 = -0.8188$ signify that these poles are located in the left-hand plane of the complex plane, suggesting the nonlinear system is stable. The small signal model shown in Fig. 2a provides insights into the linearized behavior of the system around equilibrium points with edge of chaos kernel circuit $R_1 = -3.91$ kΩ, $L_1 = -3.11$ kH, while the $ReY(i\omega; V_Q) > 0$ plot shown in Fig. 2b illustrates the stabile region. Additionally, waveform analyses of I vs. t, and x_2 vs. x_1, depict the system's response shown in Fig. 2c and d confirm its convergence to DC equilibrium and thus ensuring stability and dissipation of energy over time. These plotted analyses collectively validate the expected behavior of the PTC-NTC oscillator within the locally passive regime.

3.1.2 Edge of Chaos Kernel in Edge of Chaos Regime

The concept of the "edge of chaos" in a dynamical system suggests that within a narrow region of parameter space lies a critical zone where complex and interesting phenomena are most likely to emerge [15–18]. This region is characterized by key properties of admittance function $ReY(i\omega, V_Q) < 0$ (locally active) and real part of poles are negative (stable). In the edge of chaos regime, the system is locally

Table 2 Currents, inductances, resistances, $Re(i\omega; V_Q)$ and poles of the small-signal admittance function of the PTC-NTC memristors at different DC equilibrium voltages, V

V (V)	I (μA)	R_1 (KΩ)	L_1 (KH)	R_a (KΩ)	R_2 (KΩ)	L_2 (KH)	R_b (KΩ)	Re (iω; V_Q)	Poles
0.5	4.964	-1.624×10^3	-1.623×10^3	1	1.821×10^4	3.653×10^4	99.73	Re (iω; V_Q) > 0	−0.4987, −0.9997
1.0	10.009	-3.998×10^2	-3.993×10^2	1.001	4.442×10^3	8.983×10^3	98.91	Re (iω; V_Q) > 0	−0.4946, −0.9988
1.5	15.225	-1.731×10^2	-1.726×10^2	1.003	1.893×10^3	3.883×10^3	97.52	Re (iω; V_Q) > 0	−0.4877, −0.9972
2.0	20.714	−93.726	−93.224	1.005	1.001×10^3	2.098×10^3	95.547	Re (iω; V_Q) > 0	−0.4777, −0.9947
2.5	26.608	−57.005	−56.5	1.009	589.155	1.271×10^3	92.949	Re (iω; V_Q) > 0	−0.4643, −0.9912
3.0	33.082	−37.056	−36.549	1.014	366.342	822.353	89.669	Re (iω; V_Q) > 0	−0.4468, −0.9864
3.5	40.396	−25.022	−24.512	1.021	232.951	551.523	85.621	Re (iω; V_Q) > 0	−0.4243, −0.9795
4.0	48.961	−17.202	−16.686	1.031	147.387	375.44	80.666	Re (iω; V_Q) > 0	−0.3956, −0.9696
4.5	59.51	−11.819	−11.295	1.047	89.786	254.142	74.571	Re (iω; V_Q) > 0	−0.358, −0.9543
5.0	73.58	−7.926	−7.388	1.075	49.681	166.24	66.878	Re (iω; V_Q) > 0	−0.3067, −0.9281
5.5	119.983	−4.95	−4.38	1.139	21.071	98.558	56.416	Re (iω; V_Q) > 0	−0.2296, −0.8707
6.0	153.54	−2.499	−1.697	1.605	0.353	38.179	37.473	Re (iω; V_Q) > 0	−0.1342, −0.4814
6.1	168.135	−2.466	−1.415	2.101	1.487	42.431	39.458	Re (iω; V_Q) > 0	−0.1845 ± 0.2483i
6.209	171.553	−2.72	−1.359	2.722	1.96	44.126	40.205	Re (iω; V_Q) < 0	−0.0922 ± 0.3862i
6.30	170.269	−3.013	−1.38	3.266	1.78	43.487	39.926	Re (iω; V_Q) < 0	−0.039 ± 0.4547i
6.38820157073	167.507	−3.338	−1.426	3.825	1.402	42.122	39.319	Re (iω; V_Q) < 0	± 0.50372249i
6.5	162.963	−3.802	−1.506	4.592	0.804	39.907	38.299	Re (iω; V_Q) < 0	0.0371 ± 0.5521i
7.0	139.446	−6.593	−2.057	9.073	2.58	46.286	41.126	Re (iω; V_Q) < 0	0.0959 ± 0.6948i
7.5	118.415	−10.711	−2.853	15.716	8.284	64.187	47.62	Re (iω; V_Q) < 0	0.0372 ± 0.7999i
7.66131678261	112.582	−12.342	−3.156	18.373	10.666	71.011	49.678	Re (iω; V_Q) < 0	± 0.82930627i
8.0	101.825	−16.239	−3.858	24.762	16.501	86.805	53.804	Re (iω; V_Q) < 0	−0.0996 ± 0.8815i
8.5	89.171	−23.068	−5.031	36.075	26.971	113.19	59.248	Re (iω; V_Q) < 0	−0.2824 ± 0.9269i
9.0	79.508	−30.997	−6.328	49.339	39.259	142.375	63.857	Re (iω; V_Q) < 0	−0.4856 ± 0.9272i
9.5	72	−39.835	−7.716	64.238	52.955	173.617	67.707	Re (iω; V_Q) < 0	−0.6927 ± 0.8786i
10.0	66.031	−49.435	−9.174	80.521	67.749	206.421	70.922	Re (iω; V_Q) < 0	−0.8945 ± 0.777i
12.0	50.815	−93.773	−15.491	156.564	134.481	348.548	79.586	Re (iω; V_Q) < 0	−0.8193, −2.3652
15.0	39.194	−174.24	−26.038	296.405	249.781	585.865	86.303	Re (iω; V_Q) < 0	−0.6241, −4.041

active, meaning it is not passive but rather actively exhibits non-trivial dynamics. On the other hand, negative real part of the poles in the system's transfer function indicate that the poles are located in the left-half of the complex plane and signify the stability of nonlinear system. By combining these two conditions, the Table 2 highlighted by green color over the region 6.209 V < V < 6.38820157073 V and 7.6613678261 < V < ∞ confirm the existence of *edge of chaos regime* 1 and *edge of chaos regime* 2 respectively, which satisfy the both criteria for locally active and stable. The rows highlighted with green color in Table 2 emphasizes the fulfillment of these conditions, indicating that this region of the parameter space is where complex phenomena are likely to emerge due to the delicate balance between activity and stability. The presence of components with negative resistance and negative inductance suggest that the circuit contains an "edge of chaos kernel" operating within the edge of chaos regime which is a particular case of 2 and 3 illustrated in Table 1 for the condition of stability. This implies that even in the presence of other positive values of inductances and resistances in the small signal equivalent circuit, the PTC-NTC memristor oscillator demonstrates stable behavior as expected from locally active and stable condition.
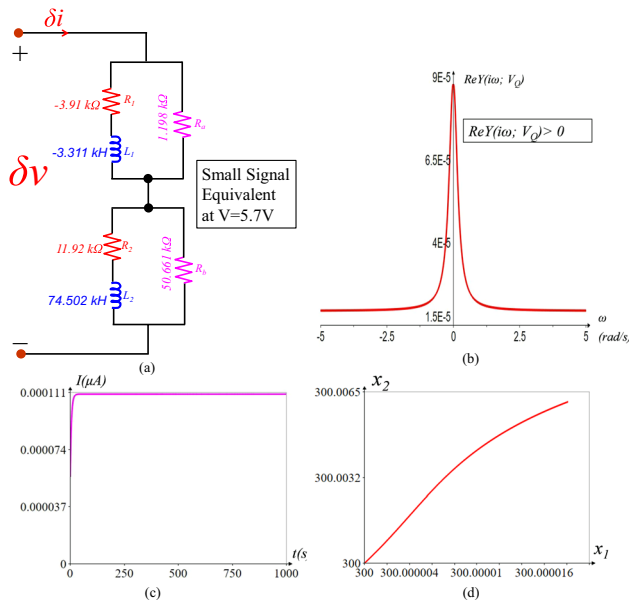
(a)

(b)

(c)

(d)

Fig. 2 a Small-signal equivalent circuit model at DC voltage V = 5.7 V in locally passive regime. **b** Small-signal admittance frequency $ReY(i\omega; V_Q)$ with respect to ω. **c** Output current (I) with respect to time. **d** Plot of x_2 vs. x_1. Observe that $R_1 = -3.91$ kΩ, $L_1 = -3.11$ kH signify the presence of edge of chaos kernel circuit and $ReY(i\omega; V_m(Q)) > 0$ illustrates the local passivity

(a)

(b)

(c)

(d)

Fig. 3 a Small-signal equivalent circuit model at DC voltage V = 6.32 V in edge of chaos regime 1. **b** small-signal admittance frequency $ReY(i\omega; V_Q)$ with respect to ω. **c** Output current (I) with respect to time. **d** Plot of x_2 vs. x_1. Please note that $R_1 = -3.083$ kΩ, $L_1 = -1.388$ kH ndicate the presence of edge of chaos kernel circuit and $ReY(i\omega; V_Q) < 0$ depicts a state of local activity

The illustration of the locally active and stable condition of the PTC-NTC oscillator in the edge of chaos regime 1 and edge of chaos regime 2 at V = 6.32 V and V = 8.58 V are shown in Figs. 3 and 4 respectively with small-signal equivalent model, plot of $ReY(i\omega; V_Q)$ vs. ω, *current* (I) vs. *time*(t), and x_2 vs. x_1. The extensive computation of the corresponding poles(p) at V = 6.32 V and V = 8.58 V, with values of $p = -0.0293 \pm 0.467$ i and $p = -0.314 \pm 0.9302$ i, respectively, indicate that these poles lie in the left-hand plane of the complex plane, implying stability. Similarly, the presence of $R_1 = -3.083$ kΩ, $L_1 = -1.388$ kH in small-signal equivalent circuit model of Fig. 3a and R1 = −24.268 kΩ, $L_1 = -5.231$ kH in small-signal equivalent circuit model of Fig. 4a signify the existence of edge of chaos kernels in the edge of chaos regime 1 and edge of chaos regime 2, respectively. Similarly, the plot of the small signal admittance function $ReY(i\omega, V_Q)$ vs. ω is negative, indicating locally active dynamics. Moreover, the waveform analyses of the *current* (I) vs. *time*(t), x_2 vs. x_1 illustrate the system's response affirming it's convergence to DC equilibrium state. These plotted analyses collectively validate the anticipated behavior of the PTC-NTC memristors oscillator in the edge of chaos regime.
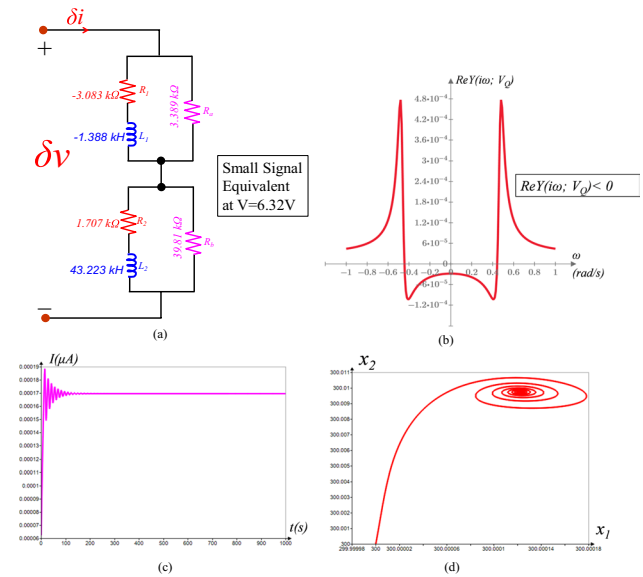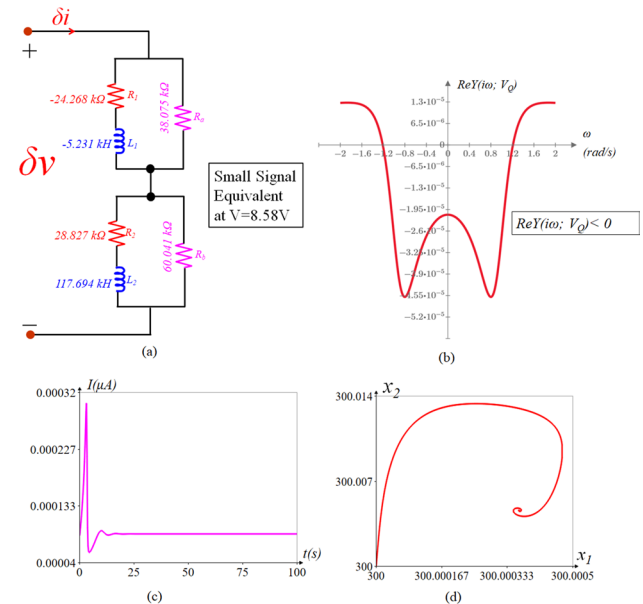

(a)

(b)

(c)

(d)

Fig. 4 a Small-signal equivalent circuit model at DC voltage V = 8.58 V in edge of chaos regime 2. **b** small-signal admittance frequency $ReY(i\omega; V_Q)$ with respect to ω. **c** Output current (I) with respect to time. **d** Plot of x_2 vs. x_1. Please note that $R_1 = -24.268$ kΩ, $L_1 = -5.231$ kH indicate the presence of edge of chaos kernel circuit and $ReY(i\omega; V_Q) < 0$ depicts a state of local activity

3.1.3 Edge of Chaos Kernel in Locally Active Unstable Regime

In a locally active unstable regime, the real part of the admittance function evaluated at a specific frequency, $Re(Y(i\omega; V_Q)) < 0$ and the real parts of the poles of the system lie in open right hand plane. The condition $Re(Y(i\omega; V_Q)) < 0$ indicates that the real part of the admittance function evaluated at a particular frequency ω is negative. This condition suggests that the system is locally active, meaning there is dynamic activity or response to perturbations, rather than being in a stable, quiescent state. Furthermore, the positive real part of the poles which lie in the open right-hand plane implies the DC equilibrium points in this regime is unstable. Therefore, within the locally active and unstable regime, complex behaviors emerge, encompassing a spectrum of dynamic phenomena such as oscillations and chaos. Table 2 highlighted by the red color between the two purely imaginary bifurcation points corresponding to poles $\pm$ 0.50372249 i and $\pm$ 0.82930627 i confirm the existence of a locally active and unstable regime. The presence of a components with negative resistance and negative inductance suggest that the circuit contains an "edge of chaos kernel" operating within the locally active and unstable regime. The combination of the edge of chaos kernel with positive inductances and resistances in the small-signal model aligns with cases 2 and 3 illustrated in Table 1 for the condition of instability. Positive values of inductances and resistances, alongside the characteristics of the edge of chaos kernel, contribute to the system's instability, creating a sinusoidal oscillation in PTC-NTC memristors.

Figure 5 depict the small-signal equivalent model, plots of $ReY(i\omega; V_Q)$ vs. t, *current (I)* vs. t, x_2 vs. x_1 at $V = 7.20$ V at the locally active and unstable regime. Extensive computations of the corresponding poles $p = 0.084 \pm 0.7393$ i at $V = 7.20$ V reveal that, these poles reside in the right half-plane of the complex plane, indicating instability. Furthermore, the presence of $R_1 = -8.072$ kΩ and $L_1 = -2.348$ kH in the small-signal equivalent circuit model signifies the existence of an edge of chaos kernel in the locally active and unstable regime. The plot of the small-signal admittance functions, $Re(Y(i\omega; V_Q))$ vs. ω exhibit negativity, indicating locally active dynamics. Moreover, waveform analyses of the I vs. t, and x_2 vs. x_1 illustrate the system's response, affirming its convergence to oscillation. These plotted analyses collectively validate the anticipated behavior of the PTC-NTC memristor oscillator in the unstable regime.

4 Application of PTC-NTC Oscillator in Voltage Control Sensing

One of the potential applications of our PTC-NTC oscillator is in the voltage control sensing circuit, as illustrated in Fig. 6. The PTC-NTC oscillator is connected to the
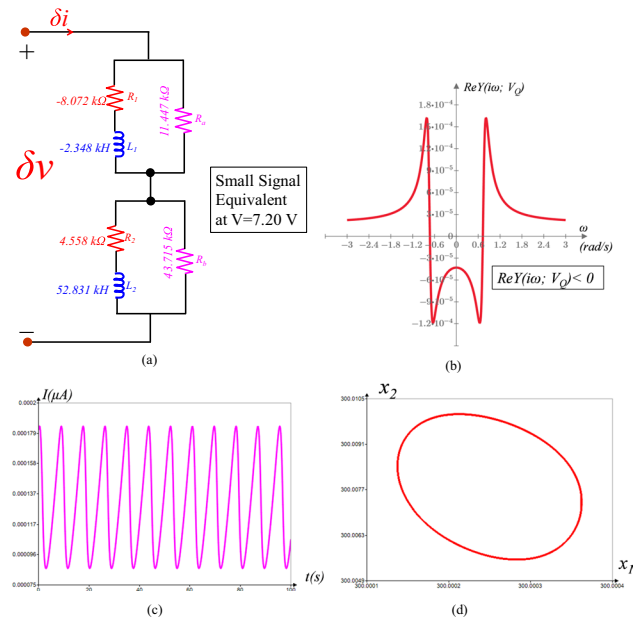

Fig. 5 a Small-signal equivalent circuit model at DC voltage V = 7.20 V in the locally active unstable regime. **b** small-signal admittance frequency $ReY(i\omega; V_Q)$ with respect to ω. **c** Output current (I) with respect to time. **d** Plot of x_2 vs. x_1. The presence of R_1 = −8.072 kΩ and L_1 = −2.348 kH in the small signal model illustrates the edge of chaos kernel circuit and $ReY(i\omega; V_Q) < 0$ depicts a state of local activity
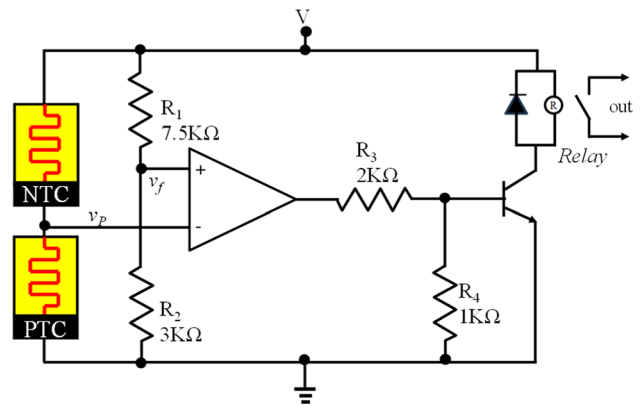

Fig. 6 Application of PTC-NTC oscillator to the voltage control sensing circuit

inverting terminal of the operational amplifier (OPAMP). When the oscillator is biased at the locally active and unstable regime over the input DC voltage 6.38820157073 < V < 7.66131678261, it generates the oscillation as discussed in the previous section. For the input DC voltage V = 7.20 V, as depicted in Fig. 7a, the change in the temperature(x_1), resistance (R_p) and voltage (v_p) of the PTC memristor is observed as shown in the Fig. 7b, c and d, respectively. The OPAMP is configured as a voltage
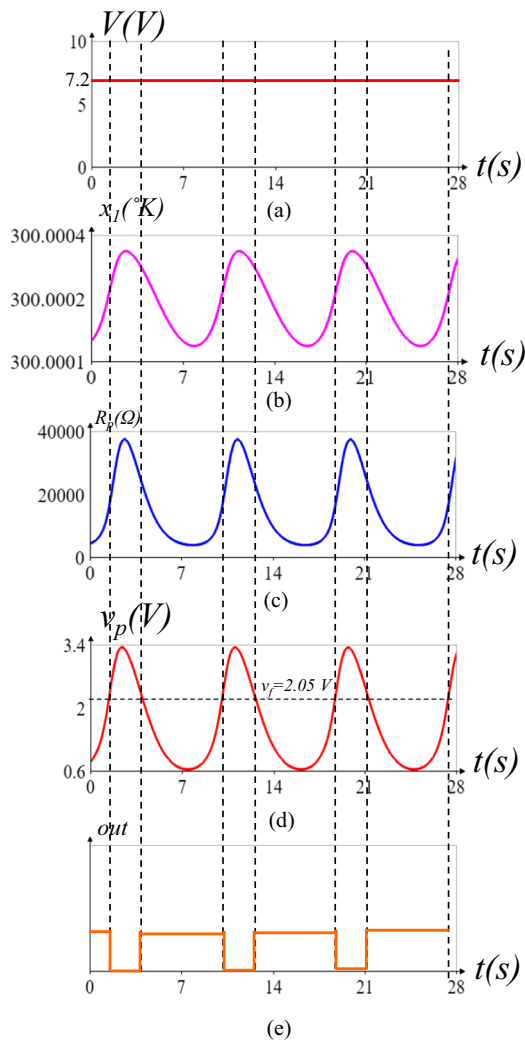
Fig. 7 Waveform of the application circuit of Fig. 6. **a** DC input voltage 7.20 V. **b** Change in the temperature of PTC memristor. **c** Change in the resistance of the PTC memristor. **d** Voltage v_p across the PTC memristor. **e** Output when the relay switch is ON

our detailed analyses, we observed how this innovative circuit pushed the boundaries of nonlinear systems from potentially stable to unstable with the addition of positive resistance or inductance, harnessing unique properties to achieve complex dynamics. We showed that the stable and periodic oscillations observed in the simplest model of memristor oscillator was not possible without the presence of *the edge of chaos kernel*. We provided compelling evidences that the *edge of chaos kernel circuit* functions as the foundational circuit for generating diverse complex dynamics in nonlinear systems. Furthermore, the application of the simplest oscillator in the voltage control sensing circuit underscores its potential contribution to scientific innovation in the field of nonlinear dynamics.

Declarations

Conflict of interest The authors declare no conflict of interest.

comparator with the reference voltage $v_f = \frac{R_2 \times V}{R_1 + R_2} = 2.05$ V applied to the non-inverting terminal. The relay turns "ON" when the voltage at point v_p is less than the voltage at point v_f. This configuration enables the circuit to function as a voltage control switch, when the output of the oscillator drops below 2.05 V, as demonstrated in Fig. 7e.

5 Conclusion

This paper introduced the memristor oscillator designed with the series connection of PTC-NTC memristors was found to be blessed by an *"edge of chaos kernel circuit"* and characterized by negative resistance and negative inductance hidden inside the small signal model. Through

References

1. Mehta VK, Mehta R (2005) Principle of electronics. S. Chand & Co., Ltd., India
2. Chua LO (1971) Memristor-the missing circuit element. IEEE Trans Circ Theory 18(5):507–519
3. Chua LO, Kang SM (1976) Memristive devices and systems. Proc IEEE 64(2):209–223
4. Itoh M, Chua LO (2008) Memristor oscillators. Int J Bifurc Chaos 18(11):3183–3206
5. Rajamani V, Yang C, Kim H, Chua L (2016) Design of a low-frequency oscillator with PTC memristor and an inductor. Int J Bifurc Chaos 26(8):1–27
6. Zhou L, You Z, Lian X, Li X (2022) A memristor-based colpitts oscillator circuit. MDPI Math 10(24):1–16
7. Anand A, Aggarwal B, Singh K (2019) Memristor based oscillator. In: International conference on computing, power and communication technologies, pp 380–384
8. Sah MP, Mannan ZI, Kim H, Chua L (2015) Oscillator made of only one memristor and one battery. Int J Bifurc Chaos 25(3):1–28
9. Chua L (2022) Hodgkin–huxley equations implies edge of chaos kernel. Jpn J Appl Phys 61(56):1–36
10. Jin P, Han N, Zhang X, Wang G (2023) Edge of Chaos Kernel and neuromorphic dynamics of a locally-active memristor. Commun Nonlinear Sci Numer Simul 117:1–25
11. Turing A (1952) The chemical basis of morphogenesis. Philos Trans R Soc Lond B 237:37–72
12. Smale S (1974) A mathematical model of two cells via Turing's equation. Am Math Soc Lect Appl Math 6:15–26
13. Galvani L (1791) De viribus electricitatis in motu musculari commentaries. Bonoiensi Sci Artium Intituo Atque Acad Comment 7:363–418
14. Adhikari SP, Sah MP, Kim H, Chua LO (2013) Three fingerprints of memristor. IEEE Trans Circ Syst I 60(11):3008–3021

15. Chua LO, Desoer CA, Kuh ES (1987) Linear and nonlinear circuits. McGraw-Hill Book Co., New York
16. Chua LO (1998) CNN: a paradigm for complexity. World Scientific, Singapore
17. Sah M, Ascoli A, Tetzlaff R, Rajamani V, Budhathoki RK (2024) Modeling excitable cells with memristors. J Low Power Electron Appl 14(2):1–36
18. Sah M, Ascoli A, Tetzlaff R, Rajamani V, Budhathoki RK (2024) Local activity principle: cause of insulin secretion by pancreatic β–cells. IEEE Trans Circ Syst I 45:789. https://doi.org/10.1109/TCSI.2024.3412732

Maheshwar Sah received the B.E. in Electronics and Communication Engineering from Nepal Engineering College, Pokhara University, Nepal in 2005. He received M.E. and PhD. in Electronics Engineering from Chonbuk National University, Republic of Korea in 2010 and 2013 respectively, where he worked as a Postdoctoral scholar from 2013 to 2014. He also worked as a Postdoctoral fellow at University of Notre Dame, Indiana, USA from 2014 to 2015. He was adjunct professor at Purdue University, Fort Wayne, Indiana, USA from 2015 to 2016. From 2015-2018, he worked as an Assistant professor at Ivy Tech, community college Indiana, USA. He is presently working as a research professor at Nepal Engineering College, Pokhara University, Nepal and Engineering standard control coordinator at TJX, Indiana, USA. His main research interests include nonlinear dynamics, analysis of memristor and memristive system, circuit design and cellular neural networks.

Vetriveeran Rajamani received his Ph.D degree in Electronics Engineering from Chonbuk National University, South Korea in 2018. He received his M.E in VLSI Design and B.E in ECE from Anna university, Chennai, in the year 2013 and 2010, respectively. He is working as an Associate professor in the School of Electronics Engineering (SENSE), Department of Micro and Nano Electronics, Vellore Institute of Technology, Vellore, Tamilnadu, India. He had published various research articles in SCI/SCIE journals, InternationalIndia. He had published various research articles in SCI/SCIE journals, International conferences, and book chapters. He is also an active member in several professional societies. He has been awarded Brain Korea (BK-21) Doctral Scholarship during the academic year 2014–2018. He was invited to give numerous guest lectures at various places in India on innovative topics. His areas of interest includes modelling of memristors, analysis and design of memristive systems in electronic and neuromorphic circuits, Analog Circuits design, Wireless Communication, Digital Signal Processing, Applied Electronics.

Ram Kaji Budhathoki received the B.E degree in Electrical and Electronic Engineering from Kathmandu University, Nepal in 2001. He received the M.E. degree in Computer Engineering from Pokhara University, Nepal in 2009 and the Ph.D degree in Electronics and Information Engineering from Chonbuk National University, Jeonju, South Korea in 2015. He has worked as a full time faculty at Nepal Engineering College, Nepal from Aug 2002 to June 2018. He is currently working as an Associate Professor in the department of Electrical and Electronics Engineering at Kathmandu University, Nepal. His current research interests include circuit design, analysis of memristor and memristive systems neural networks and electronics in agriculture.

Devaraj Somasundaram was born in Tamilnadu, India. He received the undergraduate degree in Electrical and Electronics Engineering from the Anna University Chennai, and M.Tech VLSI Design. CSIR Senior Research fellow, India and national post doctoral fellow in Indian Institute of Science, Bangalore. Previously worked as a Professor and Head of the department in SIET, Coimbatore and worked in CMR University. He completed various international funded projects sponsored by DST, ICMR and AICTE. Currently working as Associate professor in Vellore Institute of Technology, Vellore, India. His research interests are in the field of artificial intelligence, VLSI architecture for biomedical applications, Quantum computing.

Sultan Mahmood Chowdhury earned his Ph.D. degree in Electronics & Communication Engineering from National Institute of Technology Silchar, Assam, India in 2019. He received his M.Tech. degree in Communication Engineering and B.Tech. degree in Electronics & Communication Engineering from West Bengal University of Technology, India in the year 2008 and 2005 respectively. He is currently working as an Assistant Professor Sr Grade 2 in the

School of Electronics at Vellore Institute of Technology, Vellore, Tamil Nadu, India. He has also served at Malla Reddy Engineering College for Women, Secunderabad, Telangana, Veltech Rangarajan Dr. Sagunthala R&D Institute of Science and Technology, Chennai and Mallabhum Institute of Technology, West Bengal, India. He is having a teaching and research experience of more than 15 years. His current research interests include Wireless Sensor Networks and Wireless Underground Sensor Networks, Underwater Wireless Sensor Networks and Internet of Things.